Egypt. J. Chem. **Vol. 65,** No. SI: 13B pp. 137 - 144 (2022)

Egyptian Journal of Chemistry

http://ejchem.journals.ekb.eg/

Activation energy and chemical reaction effects on MHD Bingham nanofluid flow through a non-Darcy porous media

M. G. Ibrahim[a], N. F. Abdallah[b*] and M. Y. Abou-zeid[b]

[a]*Department of Basic and Applied Science, Faculty of Engineering, International academy for engineering and media science, 11311, Cairo, Egypt*

[b] *Department of Mathematics, Faculty of Education, Ain Shams University, Heliopolis, Roxy, Cairo, 11757, Egypt.*

Abstract

This study is carried out to analyze the problem of MHD mixed convection flow of Bingham nanofluid through a non-Darcy porous medium in a tube with peristalsis. Activation energy and viscous dissipation effects are taken into consideration. The governing partial differential equations are transformed into a set of nonlinear ordinary differential equations under the assumptions of long wavelength and low-Reynolds number approximations. MS-DTM technique is performed to obtain series solutions for that system of equations. The behavior of the axial velocity, temperature and nanoparticles concentration distributions under the effect of different problem parameters to these distributions is discussed analytically and graphically. Mechanics of some sophisticated physiological transports may be explained with the help of this study.

Keywords: Blood flow; Bingham nanofluid; Non-Darcian effects; Activation energy; Ms-DTM.

1. Introduction

A non-Newtonian fluid is a fluid that does not obey Newton's law of viscosity. In non-Newtonian fluids, the viscosity is affected by the forces applied to it to change its physical state to become more liquid or more solid. Many solutions of molten salts and polymers are also non-Newtonian fluids. Such as custard, honey, toothpaste, paint, blood, shower gel (shampoo) and starch **[1]**. Often, the viscosity of non-Newtonian fluids depends on the shear rate or history of the shear rate. In Newtonian fluids, the relationship between shear force and shear rate is linear, the slope of this line representing the viscosity parameter. In non-Newtonian fluids the relationship between shear stress and shear rate is different **[2]**. In this paper Bingham fluid is presented as a one of sub-classes of non-Newtonian fluid, which has numerous applications in practical part of life. Such of this applications, are ceramics **[3]**, avalanches, and muds **[4, 5]**, and shallow flow of soils **[6, 7]**. Furthermore, studies of Bingham fluid has gained more interest in the last decades, like; Tanveer et al **[8]** discretized the theoretical analysis on peristaltic flow of Bingham fluid, and they found that the distribution of nanoparticle fraction is considered as a decreasing function in thermophoretic parameter. For more details about studies of plastic and pseudoplastic fluids combined with peristaltic flow, see Refs. **[9-12].**

In chemistry and physics, activation energy is the energy that must be supplied to a chemical or nuclear system of latent reactants lead to a chemical reaction, a nuclear reaction, or various other physical phenomena. It is denoted by the symbol E_a, and the unit kilojoule/mol is used to measure it. The term was coined by the Swedish chemist Svante Arrhenius in 1889 **[13]**. Shafique et al **[14]** discretized the influences of activation energy on boundary layer flow in rotating frame; they found that the activation energy is an increasing function in temperature of fluid. Gowda et al **[15]** studied the heat and mass transfer effects on boundary layer of non-Newtonian fluid, they found that the growing values of the magnetic parameter develop the velocity gradient and decays the heat transfer. In nearly time, applications of activation energy appeared more and more in different fields like nuclear reactions in engineering **[16],** various physical

*Corresponding author e-mail: naglaa_math2019@yahoo.com ; (N. F. Abdallah).
Receive Date: 23 January 2022, Revise Date: 16 December 2022, Accept Date: 11 April 2022
DOI: 10.21608/EJCHEM.2022.117814.5310

phenomena in physics **[17,18]** and many applications can be found in Refs. **[19-23]**.

Numerous of researchers have motivated on examining different techniques to improve the fluids thermo-physical characteristics. Nanoliquids advance the heat transfer phenomenon so that new resourceful devices can be intended. These fluids are fundamentally collected of suspension of numerous kinds of nanoparticles in base fluids. Choi et al. **[24]** studied the thermal conductivity of fluids with nanoparticle. Investigational analysis of the performance of convective heat transfer of water-Al_2O_3 nanoliquid was through by Wen and Abouzeid and Ouaf **[25]** scrutinized the squeezing flow of a non-Newtonian nanoliquid between two parallel plates. The power-law nanoliquid combined with peristaltic motion a non-uniform inclined channel was deliberated by Eldabe et al. **[26]**. Recent studies and applications of nanofluid combined with blood flow can be cited in Ref. **[27–32]**.

The current scientific eagerness is to find new numerical, semi-numerical and analytical solutions of fluid problems that have a high degree of nonlinearity [**33-36**]. One of the methods that appeared to solve the problem of nonlinearity in partial or ordinary differential equations is called generalized differential transform method, which is shortened to Ms-DTM as offered through this manuscript. Differential transform method was first introduced in the end of last century by Zhou **[37]**, which is defined as a semi-analytical method for solving nonlinear partial differential equations. In early time, Odibat et al **[38]** studied the non- non-chaotic or chaotic systems by using a new modified technique that called multi-step differential transform algorithm. Furthermore, a large number of investigations have proven the effectiveness of the DTM and its modification techniques, see Refs. **[39-42]**. In other side, the main idea for Ms-DTM is to choose/ divide a suitable number of intervals from solution interval, as well as make a generalization of resulting differential transform series solution.

In the present problem, we extend the work of Tanveer et al [**8**] to include activation energy, magnetohydromagnetic, mixed convection and non-Darcian effects. Therefore, the aim of this problem is to study the effects of uniform magnetic field and viscous dissipation on flow of a Bingham nanofluid in a peristaltic tube. Brownian motion and thermophoresis effects are taken into consideration. By using the assumptions of long wavelength and low-Reynolds number, series solutions for the axial velocity, temperature, microrotation and nanoparticles distributions are obtained by using MS-DTM. The effects of pertinent parameters of the problem on these solutions are analyzed and depicted graphically.

2. Mathematical formulations

Peristaltic transport of Bingham nanofluid in a two dimensional microchannel is considered. In addition, the flow is driven by the magnetic field B_0 along the channel with d, λ and c uniform thickness, wavelength and constant speed, respectively (see Fig. 1).

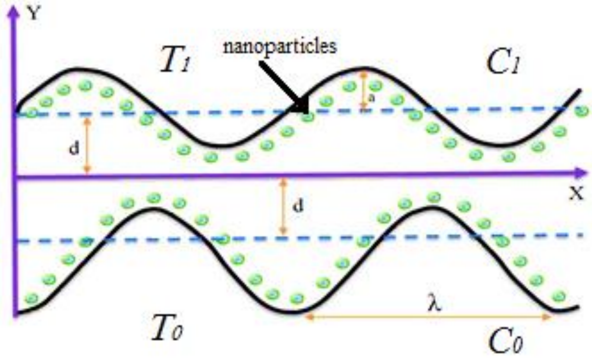

Fig.1. Physical model of problem.

Equations for wall deformation can be expressed as **[8]**

$$Y = \pm a \pm b\cos\left(\frac{2\pi}{\lambda}(\bar{X} - c\bar{t})\right) = \pm\bar{H}(\bar{X},\bar{t}) \quad (1)$$

Where a, t and b denote the amplitude, the time and the dimensional non-uniformity of the channel, respectively. Bingham fluid extra stress tensor is defined as:

$$\tau = -p\boldsymbol{I} + \boldsymbol{S}, \quad (2)$$

$$\boldsymbol{S} = \begin{cases} (\mu\dot{\gamma} + \tau_0)\boldsymbol{A}_1, & \text{for} \quad \tau \geq \tau_0 \\ \boldsymbol{A_1} = 0, & \text{for} \quad \tau > \tau_0 \end{cases}. \quad (3)$$

Where, the extra stress tensor represented by $\boldsymbol{S}$, the pressure p, the identity tensor $\boldsymbol{I}$, $\boldsymbol{A_1} = grad\bar{\boldsymbol{V}} + (grad\bar{\boldsymbol{V}})T$ is first Rivlin–Erickson tensor, $\bar{\boldsymbol{V}} = (\bar{u}(\bar{x},\bar{y},\bar{t}), \bar{v}(\bar{x},\bar{y},\bar{t}),\ 0)$ the velocity of fluid, μ the viscosity of the fluid and τ the yield stress. The governing equations of present model given as follows **[8, 13, 17]**:

$$\frac{\partial U}{\partial x} + \frac{\partial V}{\partial y} = 0, \quad (4)$$

$$\frac{\partial U}{\partial t} + U\frac{\partial U}{\partial X} + V\frac{\partial U}{\partial Y} = -\frac{\partial P}{\partial x} + \left[\frac{\partial \boldsymbol{S_{XX}}}{\partial X} + \frac{\partial \boldsymbol{S_{XY}}}{\partial Y}\right] - \rho_f C_s u\sqrt{U^2+V^2} - \left(\sigma B_0^2 + \frac{\nu}{k}\right)U + (1 - C_0)\,\rho_f g\beta(T - T_0) + (\rho_p - \rho_f)g\beta^*(C - C_0), \quad (5)$$

$$\frac{\partial V}{\partial t} + U\frac{\partial V}{\partial X} + V\frac{\partial V}{\partial Y} = -\frac{\partial P}{\partial Y} + \left[\frac{\partial \boldsymbol{S_{YX}}}{\partial X} + \frac{\partial \boldsymbol{S_{YY}}}{\partial Y}\right] - \rho_f C_s V\sqrt{U^2+V^2} - \frac{\nu}{k}V, \quad (6)$$

$$\frac{\partial T}{\partial t} + U\frac{\partial T}{\partial X} + V\frac{\partial T}{\partial Y} = -\frac{k_{nf}}{(\rho c_p)_{nf}}\left(\frac{\partial^2 T}{\partial X^2} + \frac{\partial^2 T}{\partial Y^2}\right) + \frac{\boldsymbol{S_{XY}}}{(\rho c_p)_{nf}}\left(\frac{\partial U}{\partial Y} + \frac{\partial V}{\partial X}\right) + \tau_1\left[\frac{D_T}{T_m}\left(\left(\frac{\partial T}{\partial X}\right)^2 + \left(\frac{\partial T}{\partial Y}\right)^2\right)\right] + \tau_1 D_B\left(\frac{\partial C}{\partial X}\frac{\partial T}{\partial X} + \frac{\partial C}{\partial Y}\frac{\partial T}{\partial Y}\right), \quad (7)$$

$$\rho\left(\frac{\partial C}{\partial t} + V\frac{\partial C}{\partial Y} + U\frac{\partial C}{\partial X}\right) = D_B\left(\frac{\partial^2 C}{\partial X^2} + \frac{\partial^2 C}{\partial Y^2}\right) + \frac{D_T}{T_m}\left(\frac{\partial^2 T}{\partial X^2} + \frac{\partial^2 T}{\partial Y^2}\right) - K_r^2(C - C_0)\left(\frac{T}{T_0}\right)\exp\left(\frac{E_a}{kT}\right), \quad (8)$$

Here ρ_{nf}, σ_{nf}, g, B_0, C, $(\rho C)_{np}$ and K_{nf} portrays the nanofluid density, the electrical conductivity of fluid, the gravity, the magnetic field, the concentration of nanomaterial, the effective heat capacity and the thermal conductivity of nanofluid, correspondingly. D_B is the Brownian diffusion parameter and S'_{ij} extra stress tensor components, $\tau_1 = \frac{(\rho c_p)_{nf}}{\rho c_p}$ represents the ratio of effective heat capacity of nanoliquid to heat capacity of the base fluid.

The boundary condition for the momentum equation is as follows

$$\frac{\partial u}{\partial y} = 0, \text{at } y = 0 \text{ and } u = 0, \text{at } y = \bar{H}(\bar{X}, \bar{t}) = a + b\cos\left(\frac{2\pi}{\lambda}(\bar{X} - c\bar{t})\right), \quad (9)$$

the boundary conditions for temperature and nanoparticles concentration equations are formulated as:

$$T = T_0 \text{ on } y = 0, T = T_1 \text{ on } y = h, \quad (10)$$

$$C = C_0 \text{ on } y = 0, C = C_1 \text{ on } y = h. \quad (11)$$

The following dimensionless parameters are utilized [4]

$$x = \frac{X}{\lambda}, y = \frac{Y}{d}, u = \frac{U}{c}, v = \frac{V}{c\delta}, \delta = \frac{d}{\lambda}, h = \frac{H}{d} = 1 + mx + \varepsilon \sin 2\pi(x - t), p = \frac{d^2}{c\lambda\mu_0}, M = \sqrt{\frac{\sigma_{nf}}{\mu_0}} B_0 d, R_e = \frac{\rho_{nf} c d}{\mu_0}, E = \frac{c^2}{C_{nf} T_0}, P_r = \frac{\mu_0 C_{nf}}{K_{nf}}, B_r = P_r E, G_r = \frac{\rho_{nf} g (T - T_0)\, d^2}{\mu_0 c}, G_c = \frac{\rho_{nf} g (C - C_0)\, d^2}{\mu_0 c}, N_b = \frac{\tau D_B (C - C_0)}{\nu}, \theta = \frac{(T - T_0)}{T_0}, \varphi = \frac{(C - C_0)}{C_0}, N_t = \frac{\tau D_T (T - T_0)}{\nu\, T'_m}, u = \frac{\partial \psi}{\partial y}, v = -\frac{\partial \psi}{\partial x}, E = \frac{E_a}{k T_0}, F_s = \rho_f C_s.$$

Here M denotes Hartman number, P_r is Prandtl number, Ec Eckert number, θ is the dimensionless temperature, δ is the wave number, B_r is Brinkman number, Re is Reynolds number, N_t is the thermophoresis parameter, N_b is Brownian motion parameter, R_d is the parameter thermal radiation, G_t is thermal Grashoof number, $G_r$is concentration Grashoof number and φ is the dimensionless concentration. The simplified non dimensional equations are expressed as:

$$\frac{\partial p}{\partial x} = \frac{\partial S_{xy}}{\partial y} - F_s\left(\frac{\partial \psi}{\partial y} + 1\right)^2 - \left(M^2 + \frac{1}{Da}\right)\left(\frac{\partial \psi}{\partial y} + 1\right) + G_r\,\theta + G_c\,\varphi, \quad (12)$$

$$\frac{\partial p}{\partial y} = 0, \quad (13)$$

$$\frac{\partial^2 \theta}{\partial y^2} + B_r S_{xy}\frac{\partial^2 \psi}{\partial y^2} + P_r\, N_t\left(\frac{\partial \theta}{\partial y}\right)^2 + P_r\, N_b\frac{\partial \theta}{\partial y}\frac{\partial \varphi}{\partial y} - \sigma^2 B_0^2\left(\frac{\partial \psi}{\partial y} + 1\right)^2, \quad (14)$$

$$N_b\frac{\partial^2 \varphi}{\partial y^2} + N_t\frac{\partial^2 \theta}{\partial y^2} - \xi(\rho\theta + 1)\varphi\, e^{\frac{-E}{(\rho\theta+1)}} = 0, \quad (15)$$

$$\text{Where } S_{xy} = \left(\frac{\tau_0}{\frac{\partial^2 \psi}{\partial y^2}} + \mu\right)\frac{\partial^2 \psi}{\partial y^2} \quad (16)$$

By eliminating the pressure gradient from equations (9) and (10), we have

$$\frac{\partial^2}{\partial y^2}\left(\frac{\tau_0}{\frac{\partial^2 \psi}{\partial y^2}} + \mu\right)\frac{\partial^2 \psi}{\partial y^2} - F_s\frac{\partial}{\partial y}\left(\frac{\partial \psi}{\partial y} + 1\right)^2 - M^2\frac{\partial^2 \psi}{\partial y^2} + G_r\frac{\partial \theta}{\partial y} + G_c\frac{\partial \varphi}{\partial y}, \quad (17)$$

With associated boundary conditions

$$\psi = 0, \frac{\partial^2 \psi}{\partial y^2} = \tau_0, \theta = 0, \varphi = 0 \text{ at } y = 0 \quad (18)$$

$$\psi = 0, \frac{\partial \psi}{\partial y} = 0, \theta = 1, \varphi = 1 \text{ at } y = h = 1 + a\,Cos(2\pi x) \quad (19)$$

3. Method of solution

We applied Ms-DTM in the present manuscript to solve the system of differential equations (14), (15) and (17) with appropriate boundary conditions (18) and (19). A semi-analytical solutions of differential equation can be obtained by Ms-DTM with chosen domain. In the first steps of solution to a differential equations system, we find out the solution using DTM technique. The next step, we make a generalization for the solutions obtained to treat deficiencies caused by the differential transform method.

Finally, the main improvement of the Ms-DTM is that it could be applied straight to highly non-linear systems of differential equations deprived of needful to perturbation/linearization, or other restrictive assumptions.

The general n^{th} order ordinary differential equation can be written as

$$y(t, f, f', \ldots, f^{(n)}) = 0. \quad (20)$$

This equation is subjected to the initial guess

$$f^{(k)}(0) = d_k,\ k = 0, \ldots, n - 1. \quad (21)$$

Let $f(t)$ be analytic in a domain D and let $t = t_0$ represent any point in D. The k^{th} derivative transformation of a function $f(t)$ can be defined as follows:

$$F(k) = \left(\frac{1}{k!}\right)\left[\left(\frac{d^{(k)} f(t)}{dt^{(k)}}\right)\right]_{(t=t^0)},\ \forall t \in D. \quad (22)$$

4. Results and discussion

By using the assumption of long wavelength and small Reynolds number in our problem, we analysed the entering parameters effects on the problem physical quantities, i.e., we assumed that the parameter δ is very small and more less than unity; moreover, we take the values of pertinent parameters as $M = 0.7, \mathrm{Da} = 0.4, E = 2, \tau_0 = 0.1, \mu = 0.3, \mathrm{Fs} = 0.3, G_t = 1, G_c = 1, \mathrm{Br} = 1, \mathrm{Pr} = 1, \mathrm{Nt} = 0.2, \mathrm{Nb} = 0.4,\ \rho = 0.1$. Figs. (2) and (3) give the effects of the activation energy E and the yield stress τ_0 on the axial velocity u, respectively. Equation (12) with the help of (21) and (22) is evaluated with x = 0.3 and the axial velocity is plotted versus the transverse coordinate y in these figures. It is seen from Figs. (2) and (3), that the axial velocity increases with the increasing of E, whereas it decreases as τ_0 increases in the interval $y \in [0, 0.42]$; otherwise, it decreases by increasing E and increases as τ_0 increases. Therefore, the behaviour of u in the interval y ∈ [0, 0.42] is opposite to its behaviour in the interval y ∈ [0.42, 1.3]. It is also noted that the axial velocity for different values of E and τ_0 becomes greater near the upper wall of the tube and has a maximum value after which it decreases. Moreover, the obtained curves don't intersect at the axial of tube, this is due to the boundary conditions given in (18). The effects of M and μ on the axial velocity are found to be similar to the effect of E given in Fig. (2), with the difference that the obtained curves are very close to those obtained in Fig. (2). Moreover. the effects of the other parameters are found to be similar to them; these figures are excluded here to save space. Furthermore, the result in Fig. (7) agrees with those obtained by [43-44].

Eq. (14) evaluates how the temperature distribution T varies with the transverse coordinate y. The effects of both Forschheimer number Fs and temperature Grashof number G_T on the temperature T are shown in figures (4) and (5), respectively. It is found that the temperature increases by increasing Fs, but it decreases by increasing G_T. Furthermore, the temperature is always positive and for large values of G_T, it decreases with y till a minimum value of y, after which it increases.

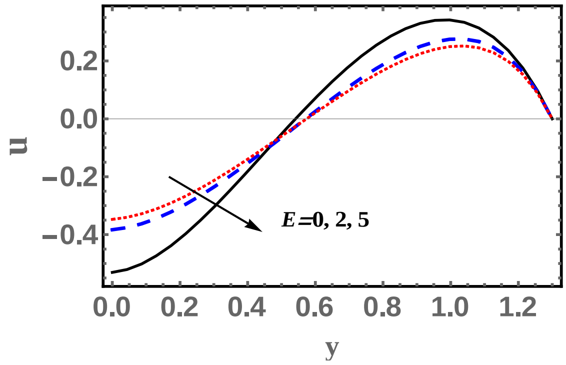

Fig. 2.

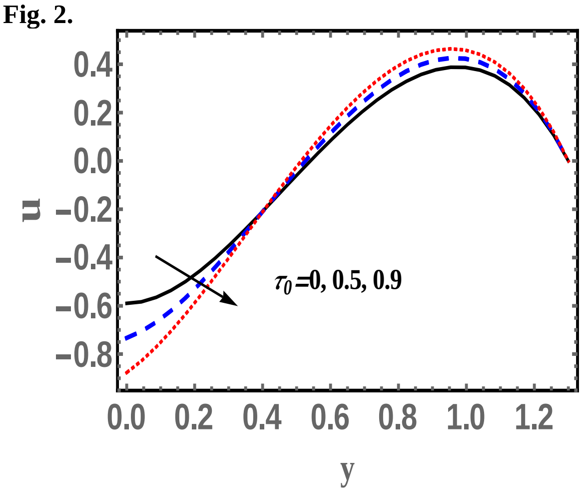

Fig. 3.

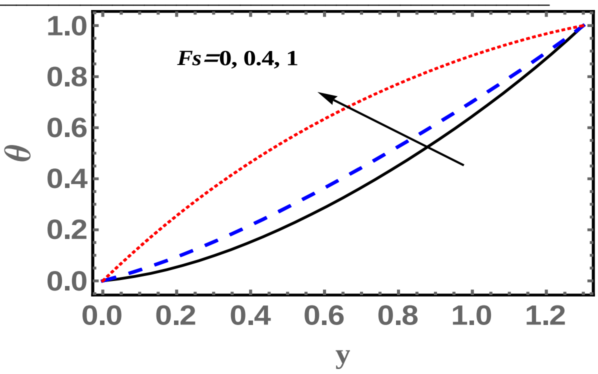

Fig. 4.

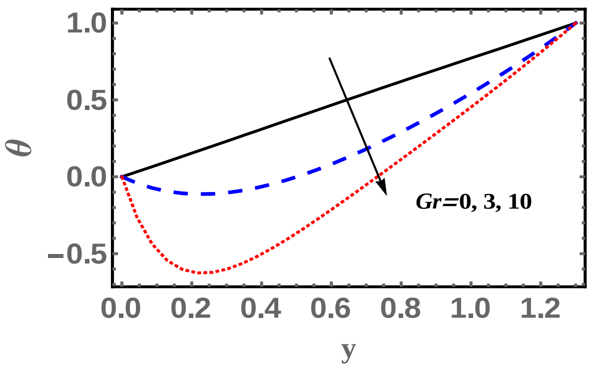

Fig. 5.

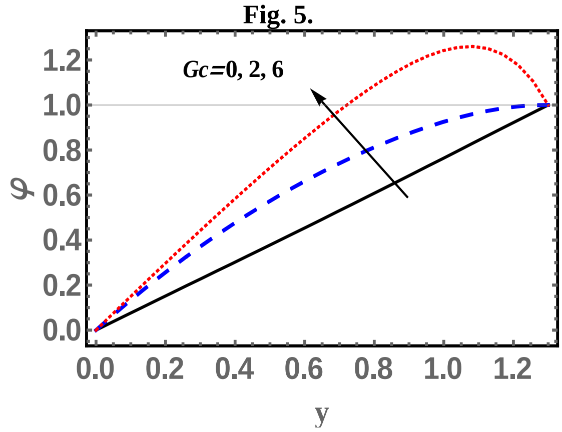

Fig. 6.

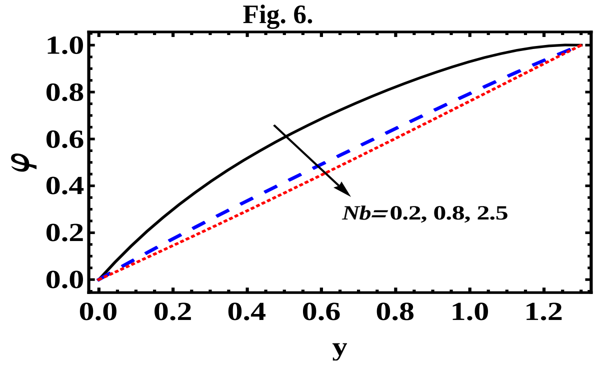

Fig. 7.

Physically, the result in Fig. (5) is due to the following: The indication of Grashof number is that it represents the ratio between the buoyancy force due to spatial variation in fluid density, which is caused by temperature distinction, to the inhibiting force due to fluid viscosity; this will lead to a reduction in fluid temperature.

Brownian motion is an indiscriminate flow of particles annotated in a fluid . This random transport agrees with the fact that the nanoparticles concentration increases or decreases with Brownian motion parameter. The effects of nanoparticles Grashof number G_f and Brownian motion parameter Nb on the nanoparticles concentration f which is a function of the transverse coordinate y are shown in Figs. (6) and (7), respectively. It is shown that the nanoparticles concentration increases as G_f increases, whereas it decreases by increasing Nb. Moreover, the nanoparticles concentration increases with y for large values of G_T, till a maximum value (at a finite value of y: $y=y_0$) after which it decreases. It is clear that the maximum of f increases by increasing G_T. In addition, the result in Fig. (7) agrees with those obtained by [45]. The effect of other parameters is found to be similar to the effect of both G_T and Nb on f, but the figures will not be given there to save space.

Trapping is treated as an interesting phenomenon related with peristaltic motion. Trapping occurs only in particular situation which is represented graphically by a large capacity ratio. The family of streamlines are specified as a fluid bolus. This bolus moves with the wave in the laboratory scope. There are an inner streams which can be determined inside the bolus. However, all the included fluid particles transfer with a mean velocity equalizing to the wave speed [46].

The spreading and size of the trapped bolus are shown in Figs. (8) and (9). These figures are depicted to reflects the advantages of the thermophoresis parameter Nt and magnetic parameter M on the streamlines. It is clear from these figures that the bolus consists of two counter – rotating vortices. In addition, the bolus size increases with the increase of Nt, while it decays in size with an enlarge in the value of the magnetic parameter M. The result in Fig. (9) is due to resistive force which is called Lorentz force. Therefore, the fluid moves slowly. That leads to reduce the size of bolus. This observed behavior agrees with the behavior noticed by [46].

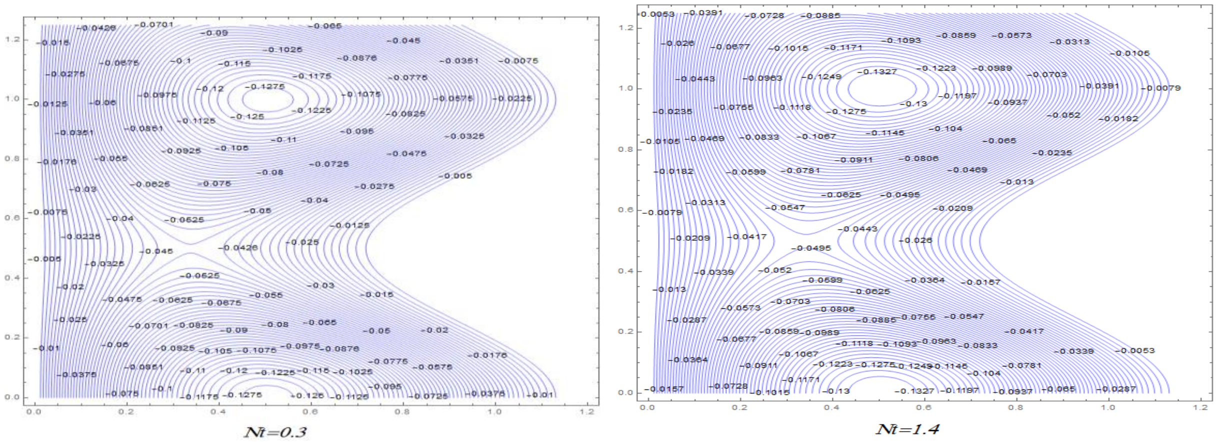

Fig. (8)

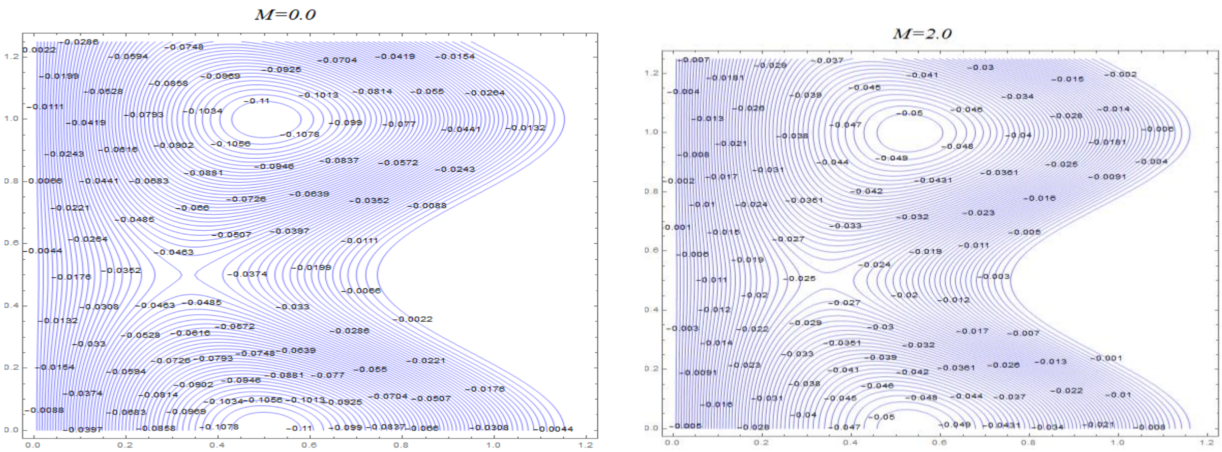

Fig. (9)

5. Conclusion

In our analysis, we extend the work of Tanveer et al [8]. So, the activation energy and viscous dissipation effect on the peristaltic flow of MHD Bingham nanofluid through a non-Darcy porous media has been analyzed. A semi-analytical expressions are constructed for the axial velocity, temperature, nanoparticles concentration distributions. Many physiological flows can be interpreted by this model. The major findings can be briefed as follows:

(1) The axial velocity *u* increases or decreases as of *Br*, *E*, *Fs* and *Da*, whereas it has an opposite behavior with each of τ_0, *Gc* and *Gt*.
(2) the axial velocity *u* becomes greater with increasing the transverse coordinate *y* and reaches maximum value (at a finite value of *y* :$y = y_0$) after which it decreases.
(3) The temperature T for different values of *Nb*, *Nt*, Fs and τ_0 increases, while, it decreases as both Gt and Gc increase.
(4) The nanoparticles concentration C has an opposite behavior compared to temperature behavior except that it has the same behavior at the channel boundary.

6 Conflicts of interest

All authors declared that there is no any conflict of interest.

7 Formatting of funding sources

Authors declared that there is no any funding source

8 Acknowledgments

M. G. Ibrahim: Writing – original draft, Visualization, Investigation, Validation **N. F. Abdallah:** Conceptualization, Methodology, Software, Data curation; **M. Y. Abou-zeid:** Validation, Writing – review & editing;

References

[1] M. Y. Abou-zeid, Homotopy perturbation method to gliding motion of bacteria on a layer of power-law nanoslime with heat transfer, J. Comput. Theor. Nanosci. 12 (2015) 3605–3614.
[2] N. T. Eldabe and M. Y. Abou-zeid, Radially varying magnetic field effect on peristaltic motion with heat and mass transfer of a non-Newtonian fluid between two co-axial tubes, Thermal Sci. 22 (6A) (2018), 2449-2458.
[3] I.R. Ionescu, Viscoplastic shallow flow equations with topography, J. Non-Newton. Fluid Mech. 193 (2013) 116–128.
[4] K.F. Liu, C.C. Mei, Roll waves on a layer of a muddy fluid flowing down a gentle slope - a Bingham model, Phys. Fluids 6 (8) (1994) 2577–2590.
[5] N. T. M. Eldabe, M. Y. Abouzeid, and H.A. Ali, Effect of heat and mass transfer on Casson fluid flow between two co-axial tubes with peristalsis, J. Adv. Res. Fluid Mech. Therm. Sci. 76(1) 2020 54-75.
[6] N. Balmforth, R. Craster and R. Sassi, Shallow viscoplastic flow on an inclined plane, J. Fluid Mech. 470 (2002) 1–29
[7] C.C. Mei and M. Yuhi, Slow flow of a Bingham fluid in a shallow channel of finite width, J. Fluid Mech. 431 (2001) 135–159.
[8] A. Tanveer , T. Salahuddin, M. Khan, M.Y. Malik and M.S. Alqarni, Theoretical analysis of non-Newtonian blood flow in a microchannel, Computer Methods and Programs in Biomedicine, 191 (2020) 105280.
[9] M. E. Ouaf and M. Y. Abou-zeid, Electromagnetic and non-Darcy effects on micropolar non-Newtonian fluid boundary-layer flow with heat and mass transfer, In. J. App. Electromagn. Mech. 66 (2021) 693-703.
[10] M.G. Ibrahim, Concentration-dependent viscosity effect on magnetonano peristaltic flow of Powell-Eyring fluid in a divergent-convergent channel, International Communications in Heat and Mass Transfer, 134, (2022), 105987.
[11] M. G. Ibrahim and H. A. Asfour, The effect of computational processingof temperature- and concentration-dependent parameters on non-Newtonian fluid MHD: Applications of numerical methods, Heat Transfer., 55, (2022) 1–18.
[12] H. M. Mansour and M. Y. Abouzeid, Heat and mass transfer effect on non-newtonian fluid flow in a non-uniform vertical tube with peristalsis, J. Adv. Res. Fluid Mech. Therm. Sci. 61 (1) (2019) 44-64.
[13] T. Salahuddin, A. M. Bashir, M. Khan and Y. Elmasry, Activation energy study for peristaltically driven divergent flow with radiation effect, Case Studies in Thermal Engineering, 27, (2021) 101172.
[14] Z. Shafique, M. Mustafa and A. Mushtaq, Boundary layer flow of Maxwell fluid in rotating frame with binary chemical reaction and activation energy, Results in Physics, 6 (2016) 627-633.
[15] R. J. P. Gowda, R. N. Kumar, A. M. Jyothi, B. C. kumara and L. E. Sarris, Impact of

binary chemical reaction and activation energy on heat and mass transfer of marangoni driven boundary layer flow of a non-Newtonian nanofluid, Processes, 2021, 9, 702.

[16] D. Borah and M.K. Baruah, Proposed novel dynamic equations for direct determination of activation energy in non-isothermal isothermal systems, Fuel processing technology, 86(2005) 781-794.

[17] Wang, Jenqdaw; Raj, Rishi, Estimate of the Activation Energies for Boundary Diffusion from Rate-Controlled Sintering of Pure Alumina, and Alumina Doped with Zirconia or Titania. Journal of the American Ceramic Society. 73 (5), (1990), 1172.

[18] A. Kiraci, H. Yurtseven, Temperature Dependence of the Raman Frequency, Damping Constant and the Activation Energy of a Soft-Optic Mode in Ferroelectric Barium Titanate. Ferroelectrics. 432 (2012) 14–21.

[19] S. Anuradha and M. Yegammai, MHD radiative boundary layer flow of nanofluid past a vertical plate with effects of binary chemical reaction and activation energy, Global Journal of Pure and Applied Mathematics, 13, 9 (2017) 6377-6392.

[20] R.K. Ameta and M. Singh, Surface tension, viscosity, apparent molal volume, activation viscous flow energy and entropic changes of water + alkali metal phosphates at T = (298.15, 303.15, 308.15) K, Journal of molecular liquids, 203(2015) 29-38.

[21] M. Mustafa, J.A. Khan, T. Hayat and A. Alsaedi, Buoyancy effects on the MHD nanofluid flow past a vertical surface with chemical reaction and activation energy, International Journal of heat and mass transfer, 108(2017) 1340-1346.

[22] L. Ahmad and M. Khan, Importance of activation energy in development of chemical covalent
bonding in flow of Sisko magneto-nanofluids over a porous moving curved surface, International Journal of Hydrogen Energy, 44(2019) 10197-10206.

[23] Y.M. Chu, M.I. Khan, Niaz B. Khan, S. Kadry, S.U. Khan, I. Tlili and M.K. Nayak, Significance of activation energy, bio-convection and magnetohydrodynamic in flow of third grade fluid (non-Newtonian) towards stretched surface: A Buongiorno model analysis, International communications in heat and mass transfer, 118 (2020) 104893.

[24] S.U.S. Choi, Enhancing thermal conductivity of fluids with nanoparticle, in: The Proceedings of the ASME. Int. Mech. Eng. Congress Exposition, ASME, San Francisco, USA, (1995), 99–105. FED 231/MD 66.

[25] M. Y. Abou-zeid and M. E. Ouaf, Hall currents effect on squeezing flow of non-Newtonian nanofluid through a porous medium between two parallel plates, Case Stud. Therm. Eng. (2021), doi: 10.1016/j.csite.2021.101362.

[26] N. T. M. Eldabe, M. Y. Abouzeid, M.A. Mohamed, and M.M. Abd-Elmoneim, MHD peristaltic flow of non-Newtonian power-law nanofluid through a non-Darcy porous medium inside a non-uniform inclined channel, Arch. Appl. Mech. 9 (2021) 1067–1077.

[27] T. Hayat, S. Qayyum, M.I. Khan, A. Alsaedi, Current progresses about probable error and statistical declaration for radiative two phase flow using ag h2o and cu h2o nanomaterials, Int. J. Hydrogen Energy 42 (2017) 29107–29120.

[28] M. Y. Abou-Zeid, Homotopy perturbation method for couple stresses effect on MHD peristaltic flow of a non-Newtonian nanofluid, Microsyst. Technol. 24 (2018) 4839-4846.

[29] M.I. Khan, A. Alsaedi, T. Hayat, N.B. Khan, Modeling and computational analysis of hybrid class nanomaterials subject to entropy generation, Comput. Meth. Prog. Biomed. 179 (2019) 104973.

[30] N. T. M. Eldabe, G. M. Moatimid, M. Abouzeid, A, A, Elshekhipy and N. F. Abdallah, Semi-analytical treatment of Hall current effect on peristaltic flow of Jeffery nanofluid, In. J. App. Electromagn. Mech. 67 (2021) 47-66.

[31] M.F. Javed, M. Waqas, M.I. Khan, N.B. Khan, R. Muhammad, M.U. Rehman, S.W. Khan, M.T. Hassan, Transport of jeffrey nanomaterial in cubic autocatalytic chemically nonlinear radiated flow with entropy generation, Appl. Nanosci. (2019), doi:10.1007/s13204-019-01071-9.

[32] N. T. M. Eldabe, G. M. Moatimid, M. Y. Abou-zeid, A. A. ElShekhipy N. F. Abdallah, A semianalytical technique for MHD peristalsis of pseudoplastic nanofluid with temperature-dependent viscosity: Application in drug delivery system. Heat Transf. - Asian Res. 49(1)(2020) 424-440.

[33] M. Y. Abou-zeid, Implicit homotopy perturbation method for MHD non-Newtonian nanofluid flow with Cattaneo-Christov heat flux due to parallel rotating disks. J. nanofluids 8 (8) (2019) 1648-1653.

[34] N. T. M. Eldabe, M.Y. Abou-zeid , O.S. Ahmed, Motion of a thin film of a fourth

grade nanofluid with heat transfer down a vertical cylinder: Homotopy perturbation method application. J. Adv. Res. Fluid. Mech. Therm. Sci. 66(2)(2020) 101-113.

[35] M. A. Mohamed, and M. Y. Abou-zeid, MHD peristaltic flow of micropolar Casson nanofluid through a porous medium between two co-axial tubes, J. Porous Media.22(9) (2019) 1079-1093.

[36] N. T. M. Eldabe, M. Y. Abou-zeid, and H.A. Ali, Effect of heat and mass transfer on Casson fluid flow between two co-axial tubes with peristalsis, J. Adv. Res. Fluid Mech. Therm. Sci. 76(1) 2020 54-75.

[37] J. K. Zhou, Differential transformation and its applications for electrical Circuits, Huazhong University Press, Wuhan, China, (in Chinese), (1986).

[38] Z.M. Odibat, Cyrille Bertelle and M. A. Aziz Alaoui, Gérard H.E. Duchamp, A multistep differential transform method and application to non-chaotic or chaotic systems, Comput. Math. Appl. 59 (2010) 1462–1472.

[39] Mostafa Nourifar, Ahmad Aftabi Sani, Ali Keyhani, Efficient multi-step differential transform method: Theory and its application to nonlinear oscillators, Commun. Nonlinear Sci. Numer. Simulat. 53 (2017) 154–183.

[40] M. Keimanesh, M.M. Rashidi, Ali J. Chamkha, R. Jafari, Study of a third grade non Newtonian fluid flow between two parallel plates using the multi-step differential transform method, Comput. Math. Appl. 62 (2011) 2871–2891.

[41] N. T. M. Eldabe, G. M. Moatimid, M. Abou-zeid, A, A, Elshekhipy and N. F. Abdallah, Instantaneous thermal-diffusion and diffusion-thermo ffects on Carreau nanofluid flow over a stretching porous sheet , J. Adv. Res. Fluid. Mech. Therm. Sci. 72 (2020) 142-157.

[42] M. Hatami, D.D. Ganji, Motion of a spherical particle on a rotating parabola using Lagrangian and high accuracy multistep differential transformation method, Powder Technol. 258 (2014) 94–98.

[43] N. T. Eldabe, M. Y. Abou-zeid, M. E. Ouaf, D. R. Mostapha and Y. M. . Mohamed, Cattaneo–Christov heat flux effect on MHD peristaltic transport of Bingham Al_2O_3 nanofluid through a non-Darcy porous medium, Int. J. Appl. Electromagn. Mech. DOI 10.3233/JAE-210057.

[44] N. T. Eldabe, M. Y. Abou-zeid, M. A. Mohamed and M. Maged, Peristaltic flow of Herschel Bulkley nanofluid through a non-Darcy porous medium with heat transfer under slip condition, Int. J. Appl. Electromagn. Mech. 66 (2021) 649-668.

[45] M. Y. Abou-zeid, A. A. Shaaban and M. Y. Alnour, Numerical treatment and global error estimation of natural convective effects on gliding motion of bacteria on a power-law nanoslime through a non-Darcy porous medium, J. Porous Media 18 (2015) 1091–1106.

[46] N. T. M. Eldabe, M. Y. Abouzeid, A. Abosaliem, A. Alana, and N. Hegazy, Homotopy perturbation approach for Ohmic dissipation and mixed convection effects on non-Newtonian nanofluid flow between two co-axial tubes with peristalsis, Int. J. Appl. Electromagn. Mech. 67 (2021) 153-163.